A Section 508–conformant HTML version of this article is available at https://doi.org/10.1289/EHP3030.

Effects of Perinatal Exposure to Dibutyltin Chloride on Fat and Glucose Metabolism in Mice, and Molecular Mechanisms, *in Vitro*

Raquel Chamorro-García,[1] Bassem M. Shoucri,[1] Sigal Willner,[1] Heidi Käch,[1] Amanda Janesick,[1] and Bruce Blumberg[1,2,3]

[1]Department of Developmental and Cell Biology, University of California, Irvine, California, USA
[2]Department of Pharmaceutical Sciences, University of California, Irvine, California, USA
[3]Department of Biomedical Engineering, University of California, Irvine, California, USA

Background: The organotin dibutyltin (DBT) is used in the manufacture of polyvinyl chloride (PVC) plastics, in construction materials, and in medical devices. Previous animal studies showed detrimental effects of DBT during *in utero* development at relatively high doses, but little was known about the effects of DBT exposure at environmentally relevant doses on endpoints such as obesity and metabolic disease.

Objectives: We tested the potential obesogenic effects of DBT using *in vitro* and *in vivo* models.

Methods. We evaluated the effects of DBT on nuclear receptor activation and adipogenic potential using human and mouse multipotent mesenchymal stromal stem cells (MSCs). We also evaluated the effects of perinatal exposure to environmentally relevant doses of DBT in C57BL/6J mice.

Results: DBT activated human and mouse PPARγ and RXRα in transient transfection assays, increased expression of adipogenic genes, promoted adipogenic differentiation and increased lipid accumulation in mouse and human MSCs, *in vitro*. DBT-induced adipogenic differentiation was abolished by the PPARγ antagonist T0070907, indicating that DBT was acting primarily through PPARγ. Perinatal exposure to low doses of DBT led to increased fat storage, decreased glucose tolerance, and increased circulating leptin levels in male, but not female, mice.

Conclusions: DBT acted as an obesogen by inducing lipid accumulation in human and mouse MSCs through a PPARγ-dependent pathway. *In vivo* exposure to biologically relevant doses of DBT during perinatal development led to increased fat storage, elevated leptin levels in plasma, and glucose intolerance in mice. Based on these findings, we posit that monitoring of DBT levels in human samples may aid in understanding and potentially preventing the rising rates of metabolic disorders in human populations. https://doi.org/10.1289/EHP3030

Introduction

In the last 30 years, there has been a dramatic increase in the incidence of obesity worldwide, not only in adults, but also in children and adolescents (Ng et al. 2014). In parallel with the increasing obesity trends, there has been an associated doubling of the incidence of diagnosed type 2 diabetes (Menke et al. 2015), which is one of the many complications linked to obesity (Kahn et al. 2006). Type 2 diabetes, the most common form of the disease, is manifested when peripheral tissues fail to properly respond to insulin, leading to elevated blood glucose. In 2011, the International Diabetes Federation estimated that around 280 million people worldwide have impaired glucose tolerance or "prediabetes"(IDF 2011). People with prediabetes have elevated blood glucose levels (fasting or glucose-challenged) that are not high enough to be considered diabetes, but that put these patients at a high risk of progressing to overt diabetes (Tabak et al. 2012). It is estimated that by 2040, around 642 million people globally will suffer from diabetes (Ogurtsova et al. 2017). Traditional factors contributing to metabolic disruption are positive energy balance (Hall et al. 2012) and genetic predisposition (Herbert 2008). However, the continuous increase in the worldwide rates of obesity in infants, children, and adolescents is not easily explained by the usually cited suite of accepted risk factors (Dabelea et al. 2014; Ogden et al. 2014) and suggests that the environment during early development may play a critical role in disease later in life (Hanson and Gluckman 2014).

Type 2 diabetes has been associated with exposure to endocrine-disrupting chemicals (EDCs) that may alter glucose homeostasis by affecting different mechanisms, such as oxidative stress or promoting adipose tissue dysfunction (Heindel et al. 2017). *In vitro* studies on human and mouse islets of Langerhans showed that environmentally relevant doses of bisphenol A (BPA) alter β-cell function via activation of estrogen receptor-beta (Soriano et al. 2012). Acute exposure to high doses of the organotin triphenyltin (TPT) disrupted β-cell function in rodents, which was reflected as a decrease in insulin secretion although no apparent morphological alteration of the pancreatic β-cells was detected (Miura et al. 1997). Alternatively, EDCs may also disturb insulin signaling of downstream pathways in target tissues such as muscle, liver, or adipose tissue (Heindel et al. 2017; Mimoto et al. 2017).

EDCs have also been causally linked to the development of obesity (Heindel et al. 2017; Keith et al. 2006; Newbold et al. 2008). Our laboratory coined the term obesogen to describe chemicals that induce abnormal fat storage *in vivo* and, therefore, may alter lipid homeostasis in the human body, leading to obesity (Grün and Blumberg 2006) An increasing list of potential obesogens, including plasticizers, pesticides, and herbicides, has been described already using both *in vitro* and *in vivo* models (reviewed in Heindel et al. 2017). One of the better-characterized obesogens is tributyltin (TBT), which activates the peroxisome proliferator–activated receptor gamma (PPARγ) and its heterodimeric partner, the retinoid X receptor alpha (RXRα) (Grün et al. 2006; Kanayama et al. 2005). Although PPARγ is considered the "master" regulator of adipogenesis (Tontonoz and Spiegelman 2008), we recently showed that signaling through RXRα, and the RXRα half of the RXRα-PPARγ heterodimer was required to commit mesenchymal stem cells (MSCs) to the adipocyte linage (Shoucri et al. 2017). *In vivo* exposure to TBT during *in utero* development in mice led to

Address correspondence to B. Blumberg, 2011 BioSci 3, Department of Developmental and Cell Biology, University of California-Irvine, Irvine, California 92697-2300, USA. Telephone: 949 824 8573. Email: blumberg@uci.edu

Supplemental Material is available online (https://doi.org/10.1289/EHP3030).

H. Käch's current address: Department of Environmental Systems Science, ETH Zurich, Zurich, Switzerland

A. Janesick's current address: Department of Otolaryngology–Head & Neck Surgery, Stanford University School of Medicine, Stanford, California, USA

B. Blumberg is a named inventor on U.S. patents 5,861,274; 6,200,802; 6,815,168; and 7,250,273 related to PPARγ.

All other authors declare they have no actual or potential competing financial interests.

Received 27 October 2017; Revised 8 April 2018; Accepted 14 April 2018; Published 21 May 2018.

Note to readers with disabilities: *EHP* strives to ensure that all journal content is accessible to all readers. However, some figures and Supplemental Material published in *EHP* articles may not conform to 508 standards due to the complexity of the information being presented. If you need assistance accessing journal content, please contact ehponline@niehs.nih.gov. Our staff will work with you to assess and meet your accessibility needs within 3 working days.

increased fat accumulation, nonalcoholic fatty liver, and a shift in the MSC compartment to favor differentiation into adipocytes at the expense of bone (Chamorro-García et al. 2013; Grün et al. 2006; Kirchner et al. 2010). Strikingly, these effects of F0 exposure were transgenerationally transmitted to at least four subsequent generations in mice (Chamorro-García et al. 2013; Chamorro-García et al. 2017). Integrative methylome, transcriptome, and chromatin accessibility analyses in both somatic tissue and germline of animals ancestrally exposed to TBT suggest that TBT may exert its transgenerational effects by eliciting changes in nuclear architecture. These changes then lead to alterations in epigenetic marks and in the transcription levels of metabolic genes that contribute to the obese phenotype (Chamorro-García et al. 2017). Taken together, these data implicate TBT and potentially its metabolites as overlooked contributors to the obesity epidemic.

The major degradation product of TBT *in vivo* is dibutyltin (DBT), which is also used industrially in the manufacture of polyvinyl chloride (PVC) plastics (Fristachi et al. 2009), used in construction materials (e.g., door and window frames, vinyl flooring, vinyl blinds, and water pipes to name a few), medical devices (e.g., tubing and packaging), and seat coverings in automobiles. DBT leaches from PVC pipes or medical tubing into the liquid they contain or transport (Sadiki et al. 1996). DBT is also found in house dust (Fromme et al. 2005; Kannan et al. 2010) and in seafood (Kannan et al. 1995; Kannan et al. 1996; Mattos et al. 2017), which suggests that human exposure may be widespread. The few human biomonitoring studies available show that the average concentration of DBT in blood is ∼4 ng/ml, or ∼16 nM (Kannan et al. 1999). The Agency for Toxic Substances & Disease Registry (ATSDR) determined the lowest-observed adverse-effect level (LOAEL) for intermediate-duration exposure (15–364 d) of DBT in rodents as 5 mg/kg/day (ATSDR 2005). After applying an uncertainty factor of 1,000 (10 for animal-to-human extrapolation, 10 for the use of LOAEL instead of the No-observed Adverse Effect Level (NOAEL), and 10 for human variability), the tolerable daily intake for humans was set at 0.005 mg/kg/day (ATSDR 2005).

In vivo studies have shown that adult exposure to relatively high doses (6 mg/kg) of DBT led to acute pancreatitis and pancreatic fibrosis in rodents (Merkord et al. 1997; Merkord et al. 1999; Zhang et al. 2016). Exposure of pregnant rats and nonhuman primates to DBT decreased fetal implantation (Ema and Harazono 2000; Ema et al. 2009) and increased fetal malformations and teratogenesis (Ema et al. 1991, 1992; Noda et al. 1993). Despite the consistency of the data showing the detrimental effect of DBT during *in utero* exposure in different animal models, the mechanism underlying these phenotypes remains largely unknown.

We first reported that DBT activated human RXRα at micromolar concentrations (Grün et al. 2006). More recently, transfection assays performed in HeLa cells showed that DBT activated PPARγ (Milton et al. 2017); however, the species from whom the gene was cloned was not specified. Studies performed using the murine preadipocyte cell line 3T3-L1 and the MSC-like mouse cell line BMS2 showed that DBT induced lipid accumulation when the cells were induced to differentiate into adipocytes (Milton et al. 2017; Yanik et al. 2011). Here we evaluated the ability of DBT to activate human and mouse PPARγ and its heterodimeric partners, human and mouse RXRα, respectively. We investigated the adipogenic effects of DBT in human and mouse MSCs and evaluated the expression of adipogenic markers, such as fatty acid binding protein-4 (FABP4), lipoprotein lipase (LPL), and fat-specific protein-27 (FSP27) in both species. We also tested the obesogenic effects of DBT *in vivo* by exposing pregnant C57BL/6J mice throughout pregnancy and lactation at dosages well below the LOAEL and measuring fat accumulation, glucose tolerance, and plasma leptin, all of which are risk factors for diabetes.

Methods

Chemicals and Reagents

TBT, DBT, dexamethasone, isobutylmethylxanthine, Nile Red, Oil Red O, Hoechst 33342, glucose, human recombinant insulin, and carboxymethylcellulose (CMC) were purchased from Sigma-Aldrich. Rosiglitazone (ROSI) was purchased from Cayman Chemicals, and T0070907 from Enzo Life Sciences. IRX194204 was a gift from Dr. Rosh Chandraratma (IO Therapeutics). Dimethylsulfoxide (DMSO) was purchased from Thermo Fisher Scientific, Inc. Calf bovine serum (CBS) was purchased from Atlanta Biologicals, and fetal bovine serum (FBS) was purchased from Gemini Bio-Products.

Transient Transfection Assays

pCMX-GAL4 (Forman et al. 1995b) and fusion constructs to nuclear receptor ligand-binding domains for mouse and human PPARγ were described previously (Forman et al. 1995a; Zhu et al. 2017). Full-length pSG5-mRXRα (a gift from Dr. Roland Schuele, University of Freiburg, Germany) and pCMX-hRXRα (Yao et al. 1993) constructs were used to test RXR activation using the reporter tk-(ApoA1)x4-luc (Blumberg et al. 1996). Transient transfections were performed in COS7 cells (ATCC® CRL-1,651™) as described (Janesick et al. 2016). Briefly, COS7 cells were seeded at 15,000 cells per well in 96-well tissue culture plates with Dulbecco's Modified Eagle Medium (DMEM; HyClone), supplemented with 10% CBS. Cells were transfected when they reached ∼90% confluency (∼24h after seeding). One microgram of effector plasmid was co-transfected with 5 μg of reporter and 5 μg of pCMX-β-galactosidase (Forman et al. 1995b) transfection control plasmids per 96-well plate in Opti-MEM® using Lipofectamine® 2000 reagent (Invitrogen™; Life Technologies), following the manufacturer's recommended protocol. After overnight incubation, the medium was replaced with DMEM supplemented with 10% resin charcoal stripped FBS plus ligands or vehicle control for an additional 24 h. DBT was tested from 10^{-10}M to 10^{-5}M, with 10^{-5}M producing noticeable cytotoxicity as judged by reduced β-galactosidase activity (Table S1). The control compounds ROSI (PPARγ agonist), IRX4204 (4204; RXR agonist), and TBT (PPARγ and RXR agonist) were tested from 10^{-10}M to 10^{-5}M. In addition, 24 h after adding the ligands to the media, cells were lysed in 165 μl of lysis buffer [25 mM Tris-phosphate (pH 7.8), 15% glycerol, 2% 3-((3-cholamidopropyl) dimethylammonio)-1-propanesulfonate (CHAPS), 1% lecithin, 1% bovine serum albumin (BSA), 4 mM ethylene glycol-bis(β-aminoethyl ether)-N,N,N′,N′-tetraacetic acid (EGTA), 6 mM Magnesium Chloride ($MgCl_2$), 1 mM dithiothreitol (DTT), 1 mM and 4-(2-aminoethyl)benzenesulfonyl fluoride hydrochloride (AEBSF)] and allowed to shake for 30 min at room temperature (RT) 22°C. For luciferase assay, 50 μl of the lysate from each well was transferred to a well in a clean, nontreated, white, flat-bottom, polystyrene, 96-well plate (Costar). Additionally, 100 μl of luciferase solution [4.28 mM magnesium carbonate hydroxide pentahydrate ($(MgCO_3)_4Mg(OH)_25H_2O$), 10.68 mM magnesium sulfate ($MgSO_4$), 80 mM Tricine (pH 7.8), 0.4 mM ethylendinitrilo tetraacetic acid (EDTA) (pH 8.0), 5 mM DTT, 0.15 mg/mL Coenzyme A, 0.5 mM adenosine triphosphate (ATP), and 0.5 mM Luciferin] made fresh was added to each well with the cell lysate, and that plate was shaken for 30 s at RT. Plates were placed in Dynatech ML3000 luminometer, and data were acquired with luminometer ML3000 (version 3.07) software. For β-galactosidase assay, 50 μl of the cell lysate was transferred to a clear, flat-bottom, 96-well plate (Thermo Fisher Scientific). In addition, 100 μl of β-galactosidase solution [60 mM sodium phosphate dibasic (Na_2HPO_4), 40 mM sodium phosphate monobasic (NaH_2PO_4), 10 mM potassium chloride (KCl), and

1 mM magnesium chloride ($MgCl_2$), 0.3% β-Mercaptoethanol, and 0.5–3 mg/mL o-nitrophenyl β-D-galactopyranoside (ONPG)] was added to each well. Plates were shaken for 30 s and incubated at RT for 15 min. Absorbance was measured with a wavelength of 405 nm on a Versamax microplate reader (Molecular Devices) and SOFTmaxPRO 4.0 software. Each luciferase read was normalized with the corresponding β-galactosidase read coming from the same transfection well and multiplied by the number of minutes the β-galactosidase plate was incubated (15 min). All transfections were performed in triplicate and reproduced in at least 4 independent experiments. Data are reported as relative light units (luciferase/β-galactosidase) or as fold induction over vehicle (0.05% DMSO) controls ± standard error of the mean (SEM) calculated using standard propagation of error (Bevington and Robison 2003).

EC_{50} and maximum activations were calculated using GraphPad Prism 7.0 (GraphPad Software, Inc.) as follows: Concentrations were transformed to logarithmic scale, and a nonlinear regression was calculated using the "log(agonist) vs. normalized response – Variable slope" function. Significance between EC_{50} for human and mouse isoforms in the presence of DBT were calculated by testing differences of best-fit values between datasets.

Adipogenic Differentiation

Mouse bone-marrow MSCs (mMSCs) were purchased from Oricell (Cyagen Biosciences), and human bone-marrow MSCs (hMSCs) were obtained from the Texas A&M Health Science Center Institute for Regenerative Medicine. Human and mouse MSCs were maintained and differentiated as described using the same media and differentiation procedure for both species (Shoucri et al. 2017). Briefly, 80,000 cells per well were seeded in a 12-well plate and maintained in DMEM supplemented with 10% CBS. When cells reached 80–90% confluency, media were replaced with differentiation media [Alpha Modification of Eagle's Medium (αMEM), 15% FBS supplemented with adipogenic induction cocktail (MDI: 500 micromolar isobutylmethylxanthine, 1 micromolar dexamethasone, 5 microgram/mL human recombinant insulin and ligands]. Specific ligands [500 nM ROSI, 50 nM TBT or DBT (1–100 nM) dissolved in DMSO] were administered every 3 d for 14 d. Antagonist assays were performed similarly, except that 100 nM T0070907 or vehicle control were added every 8 h due to the instability of the antagonist. DMSO concentrations in the medium were identical between vehicle controls and test chemicals and never exceeded 0.1%. At the end of each assay, cells were either fixed in 3.7% formaldehyde in PBS for 30 min at RT for lipid staining or homogenized in TriPure (Roche) for gene-expression analysis.

Measurement of Lipid Accumulation and mRNA Quantitation

Analyses of lipid accumulation with Nile Red and Oil Red O were performed as previously described (Chamorro-García et al. 2012; Janesick et al. 2016). Briefly, neutral lipids and nucleic acids were stained with Nile Red (1 mg/mL) and Hoechst 33342 (1 mg/mL), respectively. Total fluorescence per well was measured in a SpectraMax Gemini XS spectrofluorometer (Molecular Devices) using SoftMax Pro (Molecular Devices); Nile Red relative fluorescence units (RFU) were normalized to Hoechst RFU for each well to account for cell density. For Oil Red O staining, the same cells that were stained with Nile Red were washed with 60% isopropyl alcohol twice. Oil Red O staining solution was freshly made [3 parts of Oil Red O stock solution (0.3% (w/v) Oil Red O/isopropyl alcohol) and 2 parts of distilled water] and filtered twice to remove any precipitates. Cells were stained for 30 min following three washes with 60% isopropyl alcohol and subsequently maintained at 4°C in PBS until analyses. Cells were imaged using a Zeiss Axiovert 40 CFL microscope (Zeiss).

For reverse transcription and quantitative real time PCR (RT-QPCR), total RNA in TriPure (Roche) was isolated as recommended by the manufacturer. Complementary DNA was generated from 1 μg of DNAse-treated total RNA using transcriptor reverse transcription (Roche), according to the manufacturer's protocol. RT-QPCR was performed using Sybr Green Master Mix (Roche), and cDNA was quantitated in a Light Cycler 480 System (Roche) using primer sets listed in Table S2. Each primer set amplified a single band as determined by gel electrophoresis and melting curve analysis (Figure S1). RT-QPCR data were analyzed by the $2^{-\Delta\Delta Ct}$ method (Livak and Schmittgen 2001) relative to ribosomal protein 36B4 (a.k.a., RPLP0), normalizing to 0.1% DMSO vehicle. Error bars represent the SEM from four to six biological replicates, calculated using standard propagation of error (Bevington and Robison 2003).

Animal Maintenance and Exposure

Male and female C57BL/6J mice (7 weeks of age) were purchased from the Jackson Laboratory and housed in micro-isolator cages in a temperature-controlled room (25–28°C) with a 12-h light/dark cycle. Water and food were provided *ad libitum* unless otherwise indicated. Animals were treated humanely and with regard for alleviation of suffering. All procedures conducted in this study were approved by the Institutional Animal Care and Use Committee of the University of California, Irvine. All tissue harvesting was performed with the dissector blinded to which group the animal belonged to. At the moment of euthanasia, each mouse was assigned a code, known only to a lab member not involved in the dissection process.

We first performed a pilot experiment (set 1) in which animals were exposed to the chemicals during *in utero* development and lactation. Animals from set 1 were maintained on a standard diet (SD - Rodent Diet 20 5053*; PicoLab; 13.4% KCal from fat) throughout the experiment until euthanasia on week 8. Animals from set 2 were exposed similarly to animals from set 1 but were fed with a diet with higher fat content (HFD - Mouse Diet 20 5058*; PicoLab; 21.2% KCal from fat) from week 4 until euthanasia at week 17.

Animal numbers required for the dietary challenge were estimated using *a priori* power analyses [G*Power v3.1.5]. Based on previous data published in our laboratory (Chamorro-García et al. 2017), differences in fat content between TBT-exposed and control males when maintained with the higher fat diet (HFD) are ≥23% with SEM within groups of ≤10%. Hence, setting type I and type II errors (α and β) at 0.05 and the effect size d = 1.47, the minimum sample size required for a power (1–β) of 0.8 was calculated to be ≥7 animals per group.

Female C57BL/6J mice (8 and 12 females per treatment group for sets 1 and 2, respectively) were randomly assigned to the different treatment groups and exposed via drinking water to different concentrations of DBT (5, 50, or 500 nM), 50 nM TBT or 0.1% DMSO vehicle (all diluted in 0.5% carboxymethyl cellulose in water to maximize solubility) for 7 d prior to mating. This TBT concentration was chosen based on our previous study (Chamorro-García et al. 2013) and is 5 times lower than the established NOAEL (IPCS 1999). For DBT, we referred to the established LOAEL for intermediate exposure established by the ATSDR at 5 mg/kg/day for rodents (ATSDR 2005) and chose the highest concentration in our experiment to be 100-fold lower. Therefore, we treated the water with 500 nM, 50 nM and 5 nM, which is equivalent to 50, 5, and 0.5 μg/kg/day (100-, 1,000-, and 10,000-fold lower than the LOAEL) assuming an average body weight of 30 g and 8.5 ml of water consumption per day for a pregnant C57BL/6J female. The intermediate concentration

(5 μg/kg/day) is equivalent to the human tolerable daily intake. Chemicals were administered to the dams throughout pregnancy and lactation. Sires were never exposed to the treatment.

Chemical exposure experiments in multiparous animals can be confounded by litter effects. Standard approaches to control for such effects in gestational exposure experiments rely primarily on using litter as the experimental '*n*', or selecting one male and one female per litter as representative. However, litter size and sex ratio can affect growth trajectories and subsequent body composition, which can cause litter effects when assessing metabolic endpoints such as obesity (Suvorov and Vandenberg 2016). To avoid this potential confounder, we strictly controlled litter sizes, rejecting litters with fewer than six or more than eight animals and litters with fewer than two members of one sex. We also tested litter size and sex distribution at each chemical dose to identify whether litter effects may have occurred. We considered both male and female offspring separately in our analysis.

Body weight and body composition were measured weekly using EchoMRI™ Whole Body Composition Analyzer, which provides lean, fat, and water-content information. Total water weight includes free water mainly from the bladder and water contained in lean tissue.

Glucose and insulin tolerance tests were performed at weeks 6–7 and 14–15, for sets 1 and 2, respectively. Animals were given 2 g of glucose/kg body weight (bw), or 0.75 IU of insulin/kg bw by intraperitoneal injection after 4 h of fasting (from 8 a.m.–12 p.m.). Glucose levels were measured with Contour® blood glucose meter (Bayer) and Contour® blood glucose strips (Bayer) every 30 min for 120 min after injection.

Animals were euthanized by isofluorane exposure followed by exsanguination after 16 h fasting (overnight) at weeks 8 (set 1) and 17 (set 2). Blood was drawn from direct heart puncture into a heparinized syringe and placed in a clean tube containing protease inhibitors (Protease Inhibitor Cocktail III – Thermo Fisher Scientific). Blood was centrifuged for 10 min at 5,000 rpm at 4°C. Plasma was transferred to a clean tube, snap-frozen in liquid nitrogen, and preserved at −80°C. Leptin and insulin levels from males and females were analyzed using the Mouse Leptin and Mouse Insulin ELISA kits (Cayman Chem). Adiponectin was analyzed following the manufacturer's protocol (Thermo Fisher Scientific). Based on previous studies from our laboratory (Chamorro-García et al. 2017), hormone level changes range from 25% to 220%, depending on the hormone analyzed with SEM within groups of ≤15%. Setting the conditions as described above with an effect size d = 3.47, the minimum sample size was calculated to be three animals per group. Pancreases were isolated, fixed in 3.7% formaldehyde in PBS, embedded in paraffin, sectioned (5 μm), and stained with Masson's Trichrome at the University of California, Irvine Pathology Core.

Statistical Analyses

Statistical analysis and graphing for all figures was conducted in GraphPad Prism 7.0 (GraphPad Software, Inc.). For adipogenesis assay, one-way analysis of variance (ANOVA) followed by Dunnett's post-hoc test were conducted to compare DMSO and the different concentrations of DBT. Unpaired *t*-test was conducted to compare the positive controls ROSI and TBT with

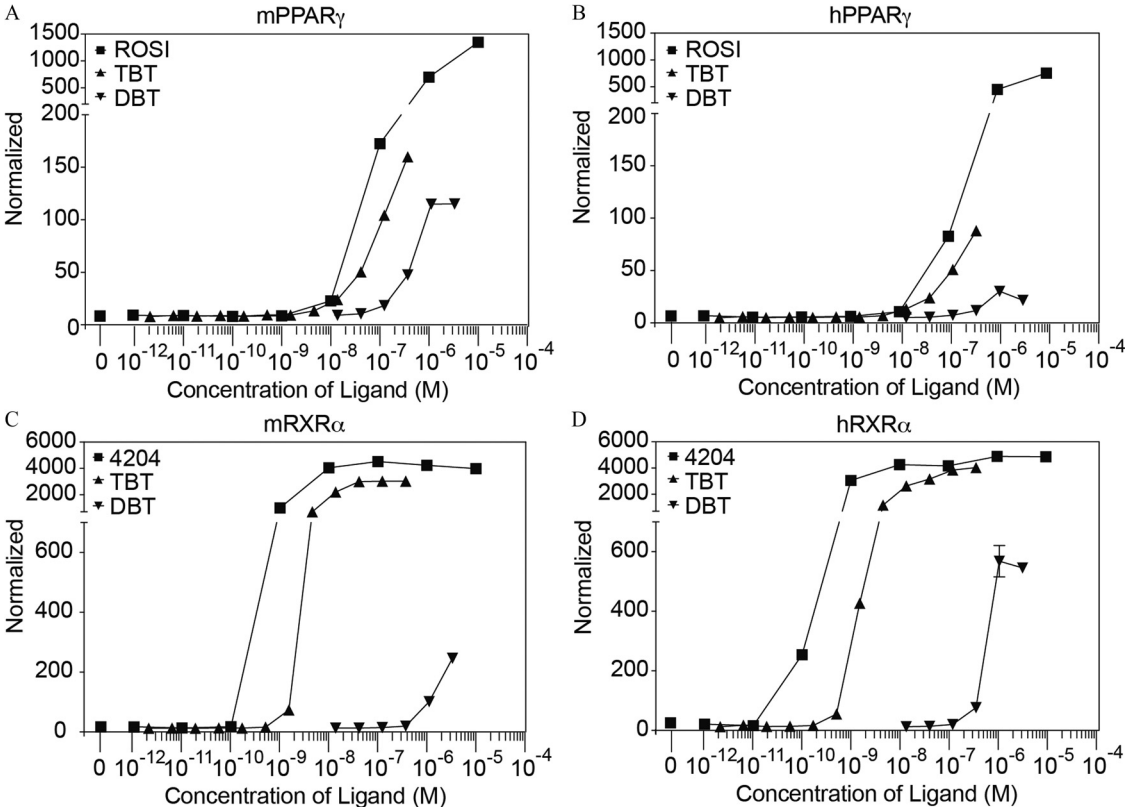

Figure 1. Activation of human and mouse isoforms of PPARγ and RXR by DBT. (A, B) Mouse and human PPARγ and (C, D) RXRα activation by increasing doses of DBT was tested in transiently transfected COS7 cells. ROSI and TBT were used as positive controls for PPARγ activation and TBT and 4204 were positive controls for RXRα activation. DBT and TBT were tested in 3-fold serial dilutions, while ROSI and 4204 were tested in 10-fold serial dilutions. Luciferase values were normalized with β-galactosidase transfection controls. Each data point represents the average of triplicates for each chemical and concentration ± SEM. Note: 4204, IRX194204; DBT, dibutyltin; DMSO, dimethylsulfoxide; M, molar; h/mPPARg, human/mouse peroxisome proliferator–activated receptor gamma; h/mRXR, human/mouse retinoid X receptor; ROSI, rosiglitazone; SEM, standard error of the mean; TBT, tributyltin.

DMSO. Student's *t*-test was performed to compare every treatment in the presence or absence of T0070907 in the antagonist assay. For longitudinal statistical analyses of body weight and body composition, and glucose and insulin tolerance tests, two-way ANOVA followed by Sidak's post-hoc test was performed to compare the different treatments. For endocrine analyses, unpaired *t*-test was conducted to compare results between treatment samples and control. $P \leq 0.05$ was considered statistically significant.

Results

DBT and Activation of Human and Mouse PPARγ and RXR in Vitro

DBT activated human and mouse PPARγ and RXRα at micromolar concentrations (Figure 1). DBT was approximately equipotent on human and mouse PPARγ ($p < 0.05$), but it was a more efficacious activator of the mouse receptor (Figure 1; Figure S2; Table S3). In contrast, DBT was a somewhat more potent ($p < 0.0001$) and efficacious activator of human RXRα than of mouse RXRα (Figure 1, Figure S2; Table S3).

DBT and Molecular Mechanisms of Lipid Accumulation in Human and Mouse MSCs

In both hMSCs and mMSCs, 100 nM DBT (but not lower concentrations) significantly increased lipid accumulation after 14 d of exposure (Figure 2A, C and Figure S3). In addition, hMSCs were more responsive to DBT than mMSCs in lipid accumulation (Fig. 2A and 2C). Therefore, 100 nM DBT was used in subsequent experiments. RT-QPCR analyses of steady state mRNA levels showed higher levels of C/EBPα and PPARγ2, which regulated each other in a positive feedback loop early in adipose differentiation (Darlington et al. 1998), in the DBT-treated MSCs than in the DMSO controls (Figure 2B, D). The levels of mRNAs encoding other adipogenic markers such as fatty acid binding protein-4 (FABP4), fat-specific protein-27 (FSP27), and lipoprotein lipase (LPL) were also higher in DBT-exposed cells (Figure 2B, D).

To determine whether the induction of lipid accumulation after DBT exposure was due to the activation of the PPARγ pathway, we tested the effect of DBT exposure in the presence and absence of the specific PPARγ antagonist T0070907. Cells exposed to 500 nM ROSI or 50 nM TBT served as positive controls for the assay because they both activate PPARγ at these doses. In hMSCs, T0070907 (100 nM) significantly blocked the ability of DBT to induce the accumulation of lipids (Figure 3A and Figure S4A). This effect was less evident in mMSCs than in hMSCs (Figure 3C and Figure S4B). Gene expression analysis of C/EBPα, PPARγ2, FABP4, LPL, and FSP27 after T0070907 treatment revealed a statistically significant decrease in steady state mRNA levels of these genes except for C/EBPα and PPARγ2 in mMSCs (Figure 3B–D).

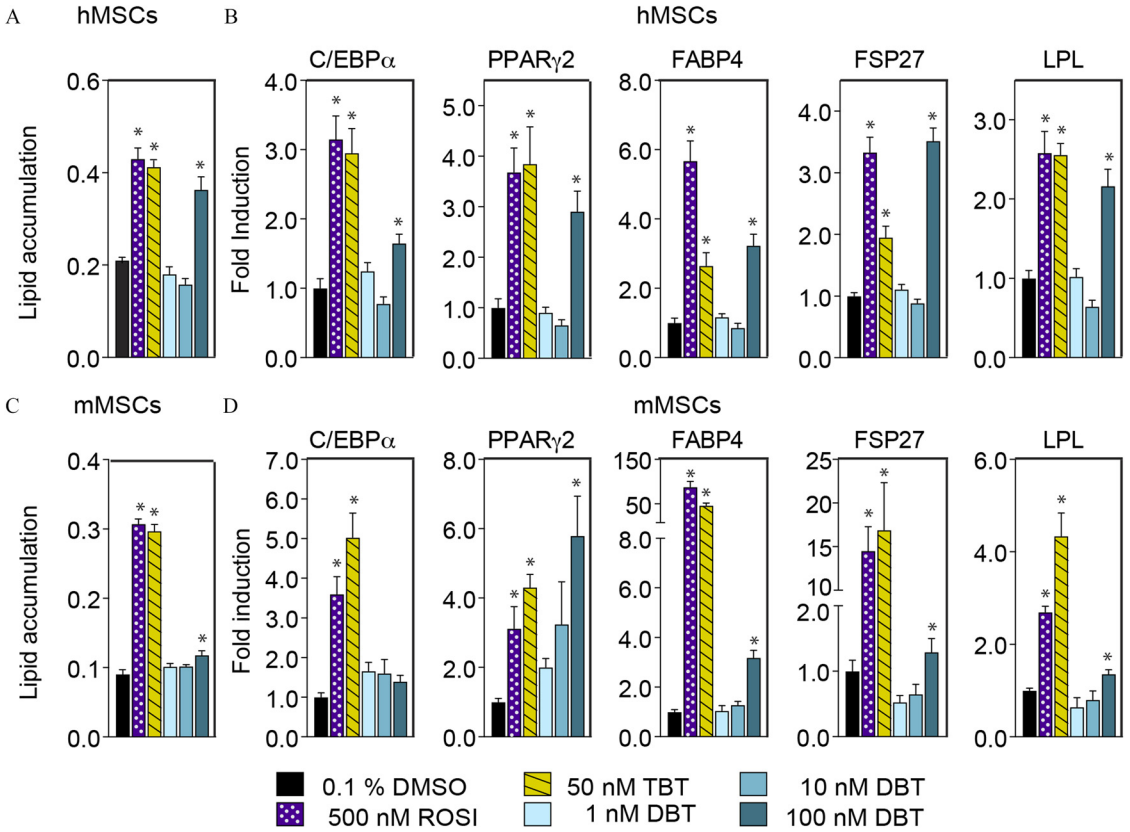

Figure 2. DBT and adipogenesis in human and mouse MSCs. Adipogenic differentiation was induced in (A, B) human and (C, D) mouse MSCs in the presence of adipogenic cocktail (MDI) and DBT (1 nM–100 nM); 500 nM ROSI and 50 nM TBT were used as positive controls and data were compared to 0.1% DMSO (vehicle). Media were replaced with fresh cocktail and ligands every 3 d for 14 d. (A, C) Graphs show lipid accumulation represented as the ratio between relative fluorescence units (RFU) of Nile Red and Hoechst. Hoechst is used to normalize lipid content to the number of cells per well. Each bar represents the average of 6 replicates ± SEM. (B, D). Gene expression is reported as fold induction over vehicle (0.1% DMSO) controls ± SEM. One-way analysis of variance (ANOVA) was conducted to compare DMSO and the different concentrations of DBT, followed by Dunnett's post-hoc test. Unpaired *t*-test was conducted for the positive controls ROSI and TBT versus vehicle. Note: C/EBPα, CCAAT/Enhancer Binding Protein Alpha; DBT, dibutyltin; DMSO, dimethylsulfoxide; Fabp4, fatty acid binding protein-4; Fsp27, fat-specific protein-27; LPL: lipoprotein lipase; h/mMSCs, human/mouse mesenchymal stem cells; PPARγ2, peroxisome proliferator–activated receptor gamma; ROSI, rosiglitazone; SEM, standard error of the mean; TBT, tributyltin. *$p \leq 0.05$ in comparison with vehicle.

Body Composition Analysis in Mice Perinatally Exposed to DBT or TBT

We consistently found a reduction in the pup survival in litters coming from dams exposed to 5 nM DBT (Table S4). Therefore, to avoid any artefactual litter effects, we removed the 5 nM treatment group from the analyses. We did not observe statistically significant differences in body weight or body composition in animals from set 1 (on standard diet) throughout the experiment (Figure 4A–B). However, we found that males from set 2 (high-fat diet) perinatally exposed to 500 nM DBT accumulated a significantly larger amount of fat than did controls (Figure 4C). The difference became apparent at 8 wk but did not reach statistical significance until 11 wk. Animals exposed to 50 nM TBT also tended to accumulate more fat than controls when exposed to the HFD, although the difference did not reach statistical significance (Figure 4C). Females did not show any significant difference in body weight or fat content (Figure 4D).

Glucose and Insulin Sensitivity in Mice Perinatally Exposed to DBT

Results of glucose and insulin tolerance tests (GTT and ITT, respectively) performed in both sets (weeks 6–7 and weeks 14–15 for sets 1 and 2, respectively) indicated no alterations in glucose or insulin tolerance in animals from set 1 (Figure 5). However, males exposed to 500 nM DBT and to the HFD (set 2) did not metabolize glucose as rapidly as control animals during the GTT (Figure 6A–B). There were no differences in glucose metabolism during the insulin tolerance test (Figure 6C–D). We did not find significant differences in glucose or insulin tolerance among females in any of the treatments (Figure 7). Fasting glucose levels were increased in the male and female animals from set 2 who were treated with 500 nM DBT, but only in female animals who were treated with 50 nM TBT (Figure 6E and Figure 7E). To test whether this effect was due to a decrease in insulin levels, we measured insulin as well as adiponectin and leptin levels in plasma from both males and females exposed to 500 nM DBT, 50 nM TBT, and controls. Leptin levels were significantly higher in males, but not in females, from both TBT and 500 nM DBT groups (Figure 6F and Figure 7F) than in DMSO controls. We did not find significant differences in insulin or adiponectin levels among groups (Figure 6F–H and Figure 7F–H). We did not find any litter bias in these results.

We evaluated pancreas histology in the DBT animals exposed to 500 nM DBT from set 2 to further characterize the glucose intolerant phenotype observed. No discernible alterations in pancreas morphology, including the numbers and sizes of islets of Langerhans were observed (Figure 8).

Discussion

The obesogens TBT and triphenyltin have been previously shown to activate both PPARγ and RXRα and to increase lipid storage in adipocytes (Grün et al. 2006; Kanayama et al. 2005). A human study showed that placental levels of TBT were directly linked to increased body weight in infants during the first 3 months after

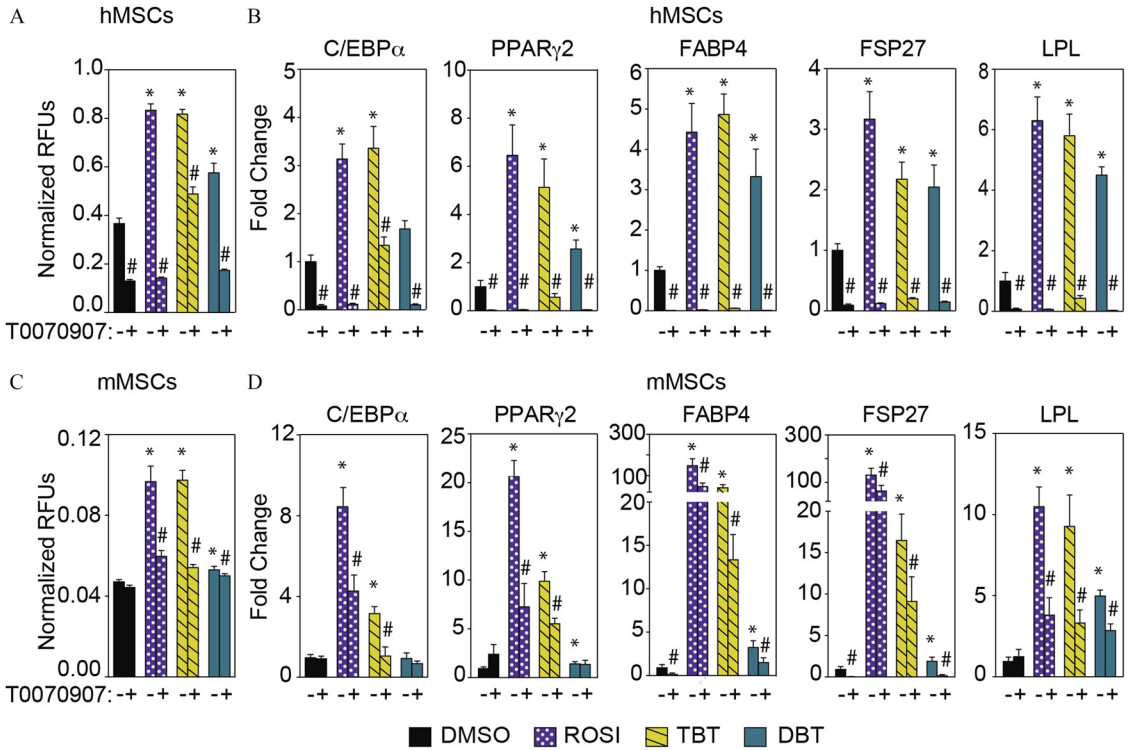

Figure 3. PPARγ antagonist T0070907 effects on DBT-induced adipogenesis in human and mouse MSCs. Adipogenesis was induced in (A, B) human and (C, D) mouse MSCs with adipogenic cocktail (MDI) and 100 nM DBT in the presence or absence of the PPARγ antagonist T0070907 (100 nM). (A, C) Lipid accumulation is presented as the ratio of relative fluorescence units (RFUs) of Nile Red and Hoechst. (B, D) Gene expression levels of adipogenic markers expressed as fold induction over vehicle. Media with adipogenic cocktail and ligands was replaced every 3 d for 14 d. Fresh T0070907 was added every 8 h throughout the experiment. One-way analysis of variance (ANOVA) was conducted to compare DMSO and the different concentrations of DBT, followed by Dunnett's post-hoc test. Unpaired *t*-test was conducted for the positive controls ROSI and TBT versus vehicle. Student's *t*-test was performed to compare every treatment in the presence or absence of T0070907. All data are expressed as the average of 6 replicates ± SEM. Note: C/EBPα, CCAAT/Enhancer Binding Protein Alpha; DBT, dibutyltin; DMSO,dimethylsulfoxide; Fabp4,fatty acid binding protein-4; Fsp27, fat-specific protein-27; LPL, lipoprotein lipase; h/mMSCs, human/mouse mesenchymal stem cells; PPARγ2, peroxisome proliferator–activated receptor gamma; ROSI, rosiglitazone; SEM, standard error of the mean; TBT, tributyltin. *$p \leq 0.05$ in comparison with vehicle (DMSO). #$p \leq 0.05$ comparing T0070907 samples with DMSO samples within the same treatment.

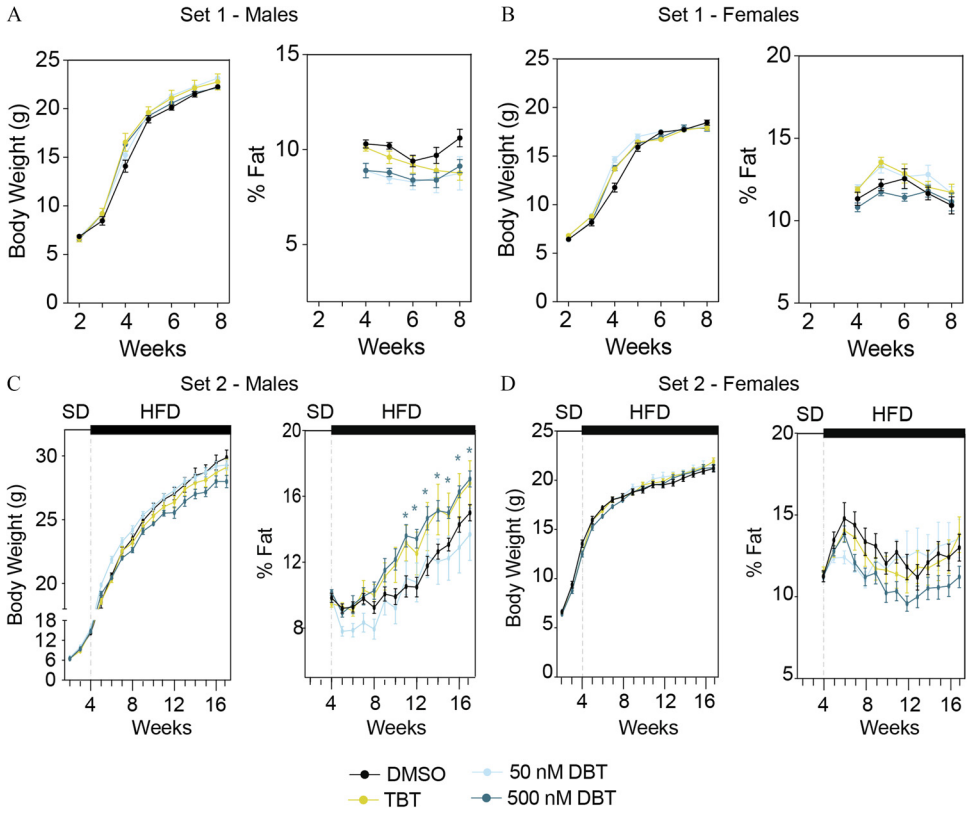

Figure 4. Body weight and fat storage in animals perinatally exposed to DBT from sets 1 and 2. Body weight and fat content in males (A, C) and females (B, D) from sets 1 (A, B) and 2 (C, D). Animals from set 1were maintained on a standard diet (SD) throughout the experiment. Animals from set 2 were maintained on SD until week 4 when their diet was switched to one with a slight increase in fat content (HFD: High fat diet). Fat content was normalized to body weight for each animal individually. Two-way analysis of variance (ANOVA) was conducted to compare DMSO and the different treatments, followed by Sidak's post-hoc test to compare treatments within each time point. $N \geqq 6$ Data are expressed as the mean ± SEM. Note: DBT, dibutyltin; DMSO, dimethylsulfoxide; TBT, tributyltin. $*p \leq 0.05$ for animals treated with 500 nM DBT compared to those treated with vehicle (DMSO).

birth (Rantakokko et al. 2014), suggesting that obesogen exposure during embryogenesis might play an important role in obesity later in life in humans. *In vivo* studies in mouse models showed that *in utero* exposure to TBT increases fat storage, promotes hepatic steatosis, and biases the MSC compartment toward the adipogenic lineage (Chamorro-García et al. 2013; Grün et al. 2006; Kirchner et al. 2010). We found that these effects were transgenerationally transmitted through the F3 (Chamorro-García et al. 2013) and the F4 generations, and recently proposed that changes in nuclear architecture caused by TBT exposure may be driving this phenotype (Chamorro-García et al. 2017).

Here we investigated potential obesogenic effects of DBT, the major *in vivo* metabolite of TBT. DBT is also widely used at high concentrations in vinyl and other forms of PVC plastics (Fristachi et al. 2009; Sadiki et al. 1996). In this study, DBT activated mouse and human PPARγ and RXRα and increased lipid accumulation in MSCs in a PPARγ-dependent manner. Perinatal exposure to DBT led to increased fat storage, glucose intolerance, and increased leptin levels in male mice when animals were challenged with a diet containing slightly higher levels of fat (21.2% vs. 13.4% KCal from fat). Males exposed to TBT did not show any alteration in glucose or insulin tolerance although they had increased levels of leptin and tended to accumulate more fat than did controls when exposed to a HFD. Although to our knowledge there are no reports concerning food intake in animals exposed to DBT, it has been reported that exposure of adult male mice to TBT reduced food intake (Bo et al. 2016). However, it was also reported in the same study that those animals developed dermatitis and hair loss during the experiment. Those observations suggest that, even though the concentration of TBT used in that study was lower than the NOAEL (0.025 mg/kg), it had a potential toxic effect affecting appetite. Therefore, we recommend that further analyses that evaluate food intake and activity after perinatal exposure to DBT be performed to establish whether DBT is affecting appetite. Females exposed to DBT or TBT also had increased fasting plasma glucose levels, although we did not detect any changes in glucose tolerance or in fat storage in comparison with controls. Because males and females are metabolically different, we speculate that differences in fat storage might become evident at older ages in females.

Leptin is an important regulator of energy and glucose homeostasis secreted by the white adipose tissue (Morton et al. 2014). The principal target of leptin is the arcuate nucleus of the hypothalamus, although other tissues such as liver can respond to leptin signaling (Ahima and Flier 2000; Morton et al. 2014). The function of leptin was initially thought to be exclusively the regulation of appetite by acting as a satiety signal following food intake (Morton et al. 2014). Leptin resistance occurs when leptin levels in obese individuals are increased, but the downstream signaling is disrupted, which includes autonomic signals to mobilize fat (Zeng et al. 2015). This disruption breaks the circuit that regulates food intake, which may lead to obesity and other metabolic disorders (Myers et al. 2010). It is now known that leptin also plays an important role in glucose homeostasis (Koch et al. 2010). Koch et al. found that in leptin-deficient mice, exogenous insulin improved glucose tolerance only in the presence of exogenous leptin, and that cells located in the arcuate nucleus were responding to the exogenous injection of both molecules (Koch et al. 2010). Their results suggest that the inhibition of the leptin-

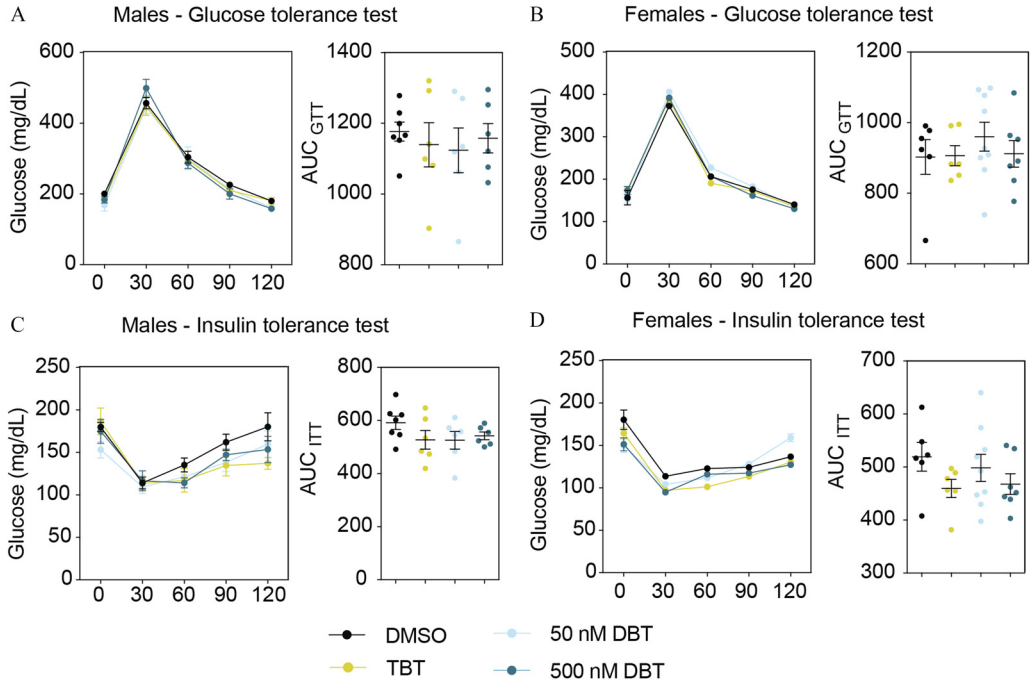

Figure 5. DBT effects on glucose homeostasis in males and females from set 1. Glucose levels and area under the curve (AUC) during glucose tolerance (A, B) and insulin tolerance (C, D) tests in males and females. Animals were fasted for 4 h prior to the test. Glucose or insulin was administered by intraperitoneal injection and glucose levels were measured every 30 min for the next 120 min. AUC was calculated for each animal independently and averaged for each treatment group. Two-way analysis of variance (ANOVA) was conducted to compare DMSO and the different treatments, followed by Sidak's post-hoc test for glucose levels at each time point. One-way ANOVA was conducted to compare DMSO and the different concentrations of DBT, followed by Dunnett's post-hoc test to compare differences in AUC. Unpaired *t*-test was conducted for TBT versus vehicle. $N \geqq 6$. Data are expressed as the mean ± SEM. Note: DBT, dibutyltin; DMSO, dimethylsulfoxide; SEM,standard error of the mean; TBT, tributyltin.

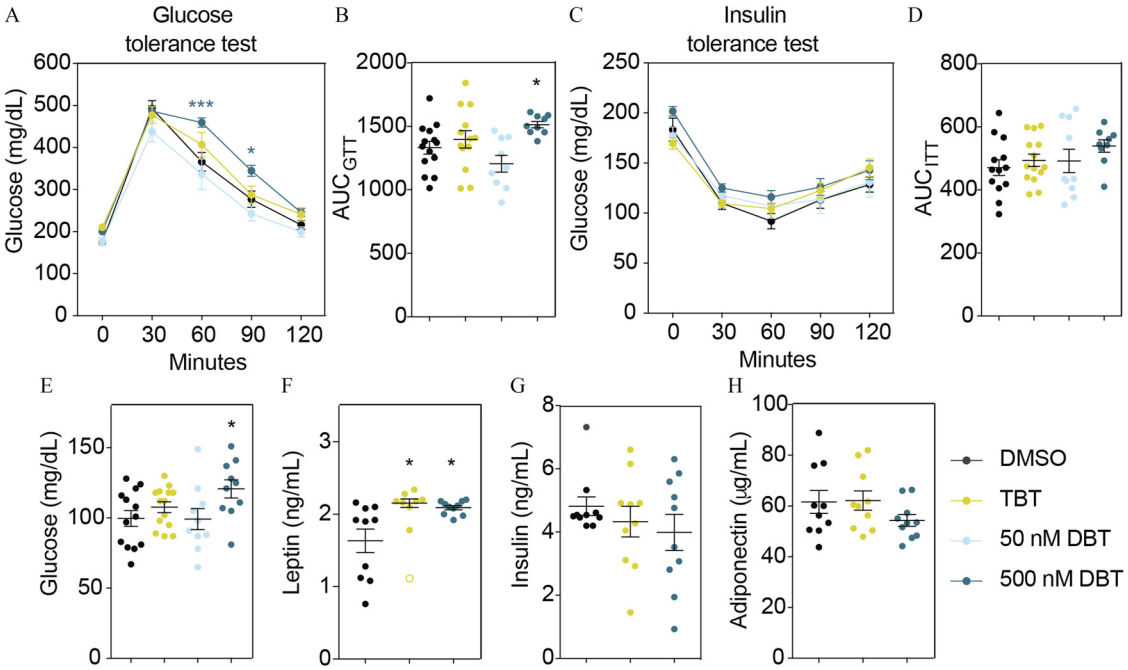

Figure 6. DBT effects on glucose homeostasis, fasting glucose, and leptin levels in males exposed to HFD. (A) Glucose levels during glucose tolerance test (GTT). (B) Area under the curve (AUC) corresponding to the GTT. (C) Glucose levels during insulin tolerance test (ITT). (D) Area under the curve (AUC) corresponding to the ITT. Animals perinatally exposed to DMSO, TBT or DBT were fasted for 4 h prior to the test. Glucose or insulin as administered by intraperitoneal injection and glucose levels were measured every 30 min for the next 120 min. AUC was calculated for each animal independently and averaged for each treatment group. (E) Glucose, (F) leptin, (G) insulin and (H) adiponectin levels after 16 h fasting. Blood was isolated by heart puncture after euthanasia and process for plasma analyses. Two-way analysis of variance (ANOVA) was conducted to compare DMSO and the different treatments, followed by Sidak's post-hoc test for glucose levels at each time point for GTT and ITT. One-way ANOVA was conducted to compare DMSO and the different concentrations of DBT, followed by Dunnett's post-hoc test to compare differences in AUC and glucose levels. Unpaired *t*-test was conducted for DMSO vs. TBT and DMSO vs. 500 nM DBT comparisons of hormones. $N \geqq 9$. Data are expressed as the mean ± SEM. Note: DBT, dibutyltin; DMSO, dimethylsulfoxide; TBT, tributyltin; SEM, standard error of the mean. $^{*}p \leq 0.05$ in comparison with vehicle (DMSO).

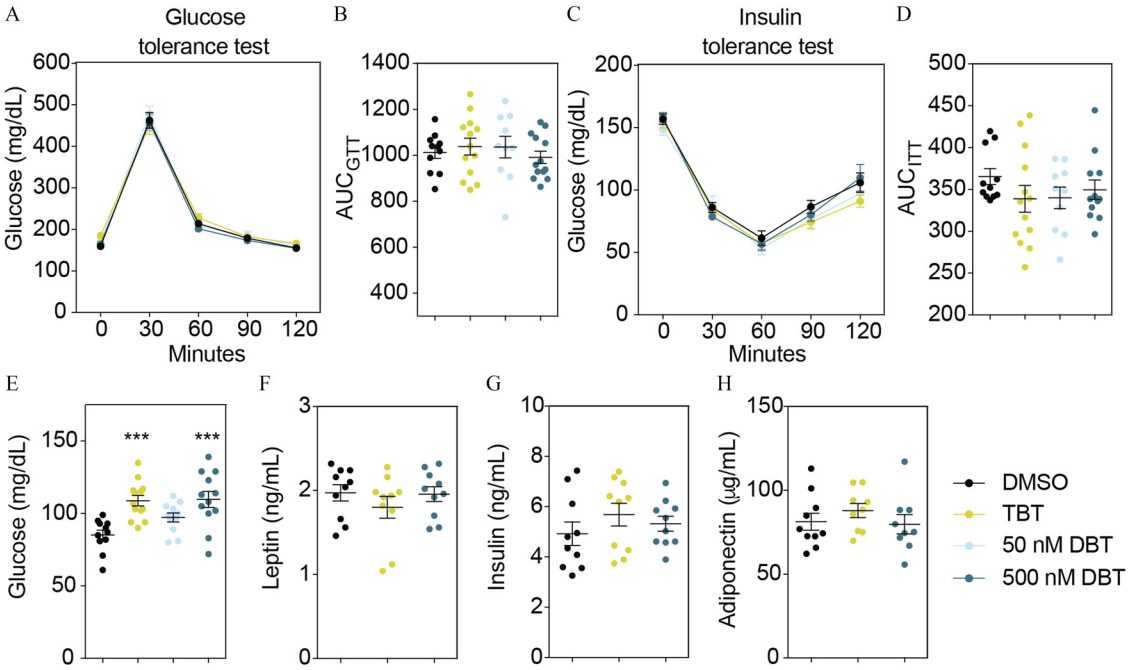

Figure 7. DBT effects on glucose homeostasis, fasting glucose, and leptin levels in females exposed to HFD. (A) Glucose levels during glucose tolerance test (GTT). (B) Area under the curve (AUC) corresponding to the GTT. (C) Glucose levels during insulin tolerance test (ITT). (D) Area under the curve (AUC) corresponding to the ITT. Animals were fasted for 4 h prior to the test. Glucose or insulin were injected by intraperitoneal injection and glucose levels were measured every 30 min for the next 120 min. AUC was calculated for each animal independently and averaged for each treatment group. (E) Glucose, (F) insulin, (G) leptin and (H) adiponectin levels after 16 h fasting. Two-way analysis of variance (ANOVA) was conducted to compare DMSO and the different treatments, followed by Sidak´s post-hoc test for glucose level at each time point. One-way ANOVA was conducted to compare DMSO and the different concentrations of DBT, followed by Dunnett's post-hoc test to compare differences in AUC and glucose levels. Unpaired *t*-test was conducted for DMSO vs. TBT and DMSO vs. 500 nM DBT comparisons for hormone levels. $N \geqq 9$ animals per group. Data are expressed as the mean ± SEM. Note: DBT, dibutyltin; DMSO, dimethylsulfoxide; TBT, tributyltin. $^{***}p \leq 0.001$ compared to vehicle (DMSO).

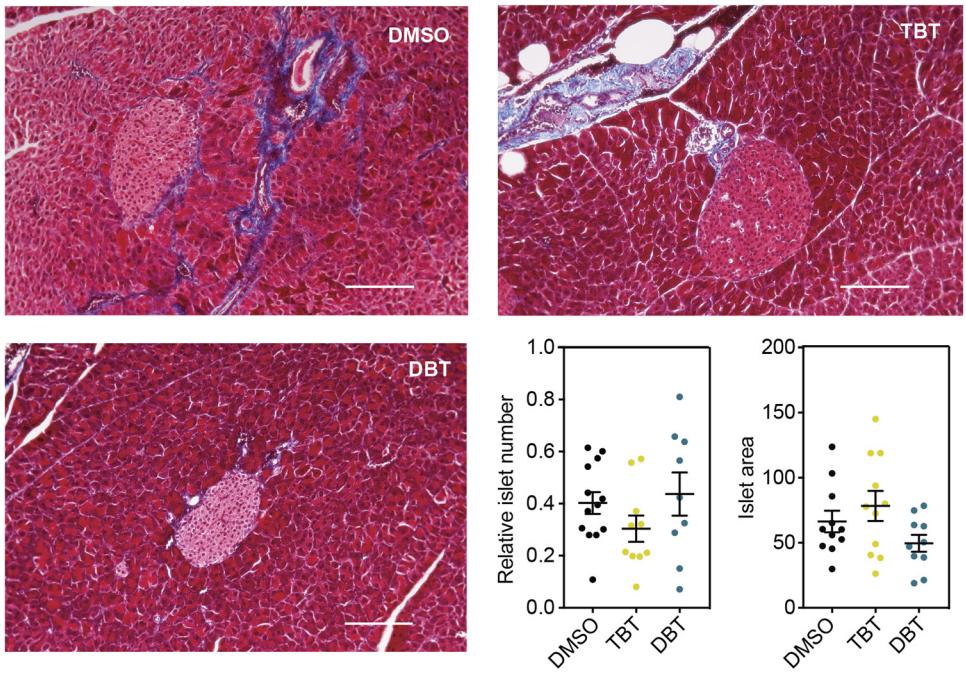

Figure 8. Analysis of pancreas morphology in males maintained on a high fat diet. Representative sections of pancreases stained with Masson's Trichrome for animals perinatally exposed to (A) DMSO, (B) TBT and (C) 500 nM DBT. (D) Average number of islets of Langerhans normalized by the area of the section. (E) Area of islets of Langerhans for each treatment in arbitrary units. Unpaired t-test was conducted for DMSO vs. TBT and DMSO vs. 500 nM DBT statistical analyses. $N \geqq 9$. Data are expressed as the mean ± SEM. Scale bar: 200 μm. Note: DBT, dibutyltin; DMSO, dimethylsulfoxide; SEM, standard error of the mean; TBT, tributyltin.

signaling pathways using leptin- and leptin receptor-deficient mice significantly reduced insulin sensitivity in the brain, which led to the disruption of glucose homeostasis (Koch et al. 2010).

We found that despite having increased leptin levels, the animals perinatally exposed to 500 nM DBT failed to metabolize glucose efficiently. However, when exogenous insulin was injected, the animals metabolized glucose at the same rate as controls, suggesting that the disturbance was not related to a lack of insulin sensitivity in peripheral tissues, such as liver, muscle, or fat. Moreover, histological analysis of the pancreas showed that overall morphology as well as the number and size of islets of Langerhans were normal in animals exposed *in utero* to 500 nM DBT in this study. These results suggest that the impaired glucose tolerance might be driven by hypothalamic leptin resistance rather than impaired β-cell insulin secretion. Taken together, we infer from these data that perinatal exposure to environmentally relevant doses of DBT led to a prediabetic phenotype in male mice. Allowing the animals to age or challenging them with diets containing a higher fat or carbohydrate content may result in progression to overt diabetes.

Prediabetes in humans is defined by elevated fasting glucose or impaired glucose metabolism following oral glucose challenge; along with obesity, prediabetes is a major risk factor for the development of type 2 diabetes and cardiovascular disease (American Diabetes Association 2017). Accepted risk factors for the development of obesity and diabetes are poor diet and lack of exercise; however, there is a growing body of evidence showing that environmental pollutants, such as obesogens and other metabolic disruptors, might be important contributors to the global diabetes epidemic (Heindel et al. 2017; Mimoto et al. 2017). A detailed evaluation of under-studied risk factors, such as obesogen exposure, in human cohorts is required to better understand the extent to which these chemicals are driving the prevalence of type 2 diabetes.

The dose of DBT at which we observed statistically significant obesogenic and prediabetic effects in our animal model was 500 nM when administered during *in utero* development and lactation via drinking water. This concentration of DBT is equivalent to a daily intake of 50 μg/kg/day (assuming an average body weight of 30 g and 8.5 ml of water consumption per day for a pregnant C57BL/6J female), which is 100-fold lower than the rodent LOAEL of 5 mg/kg/day by the ATSDR (ATSDR 2005). The ATSDR set the human tolerable daily intake at 0.005 mg/kg/day based on the rodent LOAEL. Human exposure to DBT via leaching from PVC water pipes was estimated at about 100-fold lower levels, 34 ng/kg/day (Fristachi et al. 2009). It is noteworthy that this was based exclusively on estimated exposure from a single source but did not consider possible exposure from other sources, such as house dust, food contamination, and medical devices, etc. Therefore, human daily exposure to DBT may be higher than this estimate. To the best of our knowledge, human biomonitoring for DBT (or of any organotin) levels is not currently being conducted by any public health agency.

Conclusion

In this study, we demonstrated that DBT acted as an obesogen both *in vitro* and *in vivo*. Adipogenic differentiation in exposed human and mouse MSCs exhibited increased lipid storage in cells in a PPARγ-dependent manner. *In vivo* perinatal exposure of mice to environmentally relevant doses of DBT led to increased fat storage, glucose intolerance, and increased leptin levels in males, conditions indicative of a prediabetic phenotype. These results support the hypothesis that at least one obesogen, DBT, has the potential to interact with diet to induce a prediabetic condition. To reduce and reverse the growing epidemics of obesity and related disorders such as type 2 diabetes, we suggest that human exposures to organotins such as DBT and TBT should be measured systematically to understand how they contribute to the obesity epidemic and to identify levels and sources of exposure that could be reduced or eliminated in the future.

Acknowledgments

This work was supported by grants from NIH (ES023316, ES015849, ES015849-03S1). The authors thank all members of the Blumberg laboratory for their technical assistance and Dr. Rosh Chandraratna (IO Therapeutics, Santa Ana, CA) for a gift of IRX194204, and Dr. Roland Schuele (University of Freiburg, Germany) for a gift of the plasmid pSG5-mRXRα.

References

Ahima RS, Flier JS. 2000. Leptin. Annu Rev Physiol 62:413–437, PMID: 10845097, https://doi.org/10.1146/annurev.physiol.62.1.413.

American Diabetes Association. 2017. 2. Classification and diagnosis of diabetes. Dia Care 40(Supplement 1):S11–S24, https://doi.org/10.2337/dc17-S005.

ATSDR (Agency for Toxic Substances & Disease Registry). 2005. *Toxicological profile for tin and tin compounds*.

Bevington PR, Robison DK. 2003. *Data reduction and error analysis for the physical sciences*. New York:McGraw-Hill Education.

Blumberg B, Bolado J Jr, Derguini F, Craig AG, Moreno TA, Chakravarti D, et al. 1996. Novel retinoic acid receptor ligands in Xenopus embryos. Proc Natl Acad Sci USA U S A93(10):4873–4878, PMID: 8643496, https://doi.org/10.1073/pnas.93.10.4873.

Bo E, Farinetti A, Marraudino M, Sterchele D, Eva C, Gotti S, et al. 2016. Adult exposure to tributyltin affects hypothalamic neuropeptide Y, Y1 receptor distribution, and circulating leptin in mice. Andrology 4(4):723–734, PMID: 27310180, https://doi.org/10.1111/andr.12222.

Chamorro-García R, Kirchner S, Li X, Janesick A, Casey SC, Chow C, et al. 2012. Bisphenol A diglycidyl ether induces adipogenic differentiation of multipotent stromal stem cells through a peroxisome proliferator-activated receptor gamma-independent mechanism. Environ Health Perspect 120(7):984–989, PMID: 22763116, https://doi.org/10.1289/ehp.1205063.

Chamorro-García R, Sahu M, Abbey RJ, Laude J, Pham N, Blumberg B. 2013. Transgenerational inheritance of increased fat depot size, stem cell reprogramming, and hepatic steatosis elicited by prenatal exposure to the obesogen tributyltin in mice. Environ Health Perspect 121(3):359–366, PMID: 23322813, https://doi.org/10.1289/ehp.1205701.

Chamorro-García R, Diaz-Castillo C, Shoucri BM, Käch H, Leavitt R, Shioda T, et al. 2017. Ancestral perinatal obesogen exposure results in a transgenerational thrifty phenotype in mice. Nat Commun 8(1):2012, PMID: 29222412, https://doi.org/10.1038/s41467-017-01944-z.

Dabelea D, Mayer-Davis EJ, Saydah S, Imperatore G, Linder B, Divers J, et al. 2014. Prevalence of type 1 and type 2 diabetes among children and adolescents from 2001 to 2009. JAMA 311(17):1778–1786, PMID: 24794371, https://doi.org/10.1001/jama.2014.3201.

Darlington GJ, Ross SE, MacDougald OA. 1998. The role of C/EBP genes in adipocyte differentiation. J Biol Chem 273(46):30057–30060, PMID: 9804754.

Ema M, Itami T, Kawasaki H. 1991. Teratogenicity of di-n-butyltin dichloride in rats. Toxicol Lett 58(3):347–356, PMID: 1957330.

Ema M, Itami T, Kawasaki H. 1992. Susceptible period for the teratogenicity of di-n-butyltin dichloride in rats. Toxicology 73(1):81–92, PMID: 1589881.

Ema M, Harazono A. 2000. Adverse effects of dibutyltin dichloride on initiation and maintenance of rat pregnancy. Reprod Toxicol 14(5):451–456, PMID: 11020655.

Ema M, Arima A, Fukunishi K, Matsumoto M, Hirata-Koizumi M, Hirose A, et al. 2009. Developmental toxicity of dibutyltin dichloride given on three consecutive days during organogenesis in cynomolgus monkeys. Drug Chem Toxicol 32(2):150–157, PMID: 19514951, https://doi.org/10.1080/01480540802594327.

Forman BM, Tontonoz P, Chen J, Brun RP, Spiegelman BM, Evans RM. 1995a. 15-Deoxy-delta 12, 14-prostaglandin J2 is a ligand for the adipocyte determination factor PPARgamma. Cell 83(5):803–812, PMID: 8521497, https://doi.org/10.1016/0092-8674(95)90193-0.

Forman BM, Umesono K, Chen J, Evans RM. 1995b. Unique response pathways are established by allosteric interactions among nuclear hormone receptors. Cell 81(4):541–550, PMID: 7758108, https://doi.org/10.1016/0092-8674(95)90075-6.

Fristachi A, Xu Y, Rice G, Impellitteri CA, Carlson-Lynch H, Little JC. 2009. Using probabilistic modeling to evaluate human exposure to organotin in drinking water transported by polyvinyl chloride pipe. Risk analysis: an official publication of the Society for Risk Analysis 29(11):1615–1628, https://doi.org/10.1111/j.1539-6924.2009.01307.x.

Fromme H, Mattulat A, Lahrz T, Rüden H. 2005. Occurrence of organotin compounds in house dust in Berlin (Germany). Chemosphere 58(10):1377–1383, PMID: 15686755, https://doi.org/10.1016/j.chemosphere.2004.09.092.

Grün F, Blumberg B. 2006. Environmental obesogens: organotins and endocrine disruption via nuclear receptor signaling. Endocrinology 147(6 Suppl):S50–S55, PMID: 16690801, https://doi.org/10.1210/en.2005-1129.
Grün F, Watanabe H, Zamanian Z, Maeda L, Arima K, Cubacha R, et al. 2006. Endocrine-disrupting organotin compounds are potent inducers of adipogenesis in vertebrates. Mol Endocrinol 20(9):2141–2155, PMID: 16613991, https://doi.org/10.1210/me.2005-0367.
Hall KD, Heymsfield SB, Kemnitz JW, Klein S, Schoeller DA, Speakman JR. 2012. Energy balance and its components: implications for body weight regulation. Am J Clin Nutr 95(4):989–994, PMID: 22434603, https://doi.org/10.3945/ajcn.112.036350.
Hanson MA, Gluckman PD. 2014. Early developmental conditioning of later health and disease: physiology or pathophysiology?. Physiol Rev 94(4):1027–1076, PMID: 25287859, https://doi.org/10.1152/physrev.00029.2013.
Heindel JJ, Blumberg B, Cave M, Machtinger R, Mantovani A, Mendez MA, et al. 2017. Metabolism disrupting chemicals and metabolic disorders. Reprod Toxicol 68:3–33, PMID: 27760374, https://doi.org/10.1016/j.reprotox.2016.10.001.
Herbert A. 2008. The fat tail of obesity as told by the genome. Curr Opin Clin Nutr Metab Care 11(4):366–370, PMID: 18541993, https://doi.org/10.1097/MCO.0b013e3283034990.
IDF (International Diabetes Foundation). 2011. *IDF Diabetes Atlas*, 5th ed. Brussels, Belgium: International Diabetes Federation.
IPCS (International Programme on Chemical Safety). 1999. *Concise international chemical assessment document 14, tributyltin oxide*. World Health Organization, Geneva, Switzerland.
Janesick AS, Dimastrogiovanni G, Vanek L, Boulos C, Chamorro-García R, Tang W, et al. 2016. On the utility of ToxCast™ and ToxPi as methods for identifying new obesogens. Environ Health Perspect 124(8):1214–1226, PMID: 26757984.
Kahn SE, Hull RL, Utzschneider KM. 2006. Mechanisms linking obesity to insulin resistance and type 2 diabetes. Nature 444(7121):840–846, PMID: 17167471, https://doi.org/10.1038/nature05482.
Kanayama T, Kobayashi N, Mamiya S, Nakanishi T, Nishikawa J. 2005. Organotin compounds promote adipocyte differentiation as agonists of the peroxisome proliferator-activated receptor gamma/retinoid x receptor pathway. Mol Pharmacol 67(3):766–774, PMID: 15611480, https://doi.org/10.1124/mol.104.008409.
Kannan K, Tanabe S, Iwata H, Tatsukawa R. 1995. Butyltins in muscle and liver of fish collected from certain Asian and Oceanian countries. Environ Pollut 90(3):279–290, PMID: 15091461.
Kannan K, Corsolini S, Focardi S, Tanabe S, Tatsukawa R. 1996. Accumulation pattern of butyltin compounds in dolphin, tuna, and shark collected from Italian coastal waters. Arch Environ Contam Toxicol 31(1):19–23, PMID: 8687986, https://doi.org/10.1007/BF00203903.
Kannan K, Senthilkumar K, Giesy J. 1999. Occurrence of butyltin compounds in human blood. Environ Sci Technol 33(10):1776–1779, https://doi.org/10.1021/es990011w.
Kannan K, Takahashi S, Fujiwara N, Mizukawa H, Tanabe S. 2010. Organotin compounds, including butyltins and octyltins, in house dust from Albany, New York, USA. Arch Environ Contam Toxicol 58(4):901–907, PMID: 20379706, https://doi.org/10.1007/s00244-010-9513-6.
Keith SW, Redden DT, Katzmarzyk PT, Boggiano MM, Hanlon EC, Benca RM, et al. 2006. Putative contributors to the secular increase in obesity: exploring the roads less traveled. Int J Obes (Lond) 30(11):1585–1594, PMID: 16801930, https://doi.org/10.1038/sj.ijo.0803326.
Kirchner S, Kieu T, Chow C, Casey S, Blumberg B. 2010. Prenatal exposure to the environmental obesogen tributyltin predisposes multipotent stem cells to become adipocytes. Mol Endocrinol 24(3):526–539, PMID: 20160124, https://doi.org/10.1210/me.2009-0261.
Koch C, Augustine RA, Steger J, Ganjam GK, Benzler J, Pracht C, et al. 2010. Leptin rapidly improves glucose homeostasis in obese mice by increasing hypothalamic insulin sensitivity. J Neurosci 30(48):16180–16187, PMID: 21123564, https://doi.org/10.1523/JNEUROSCI.3202-10.2010.
Livak KJ, Schmittgen TD. 2001. Analysis of relative gene expression data using real-time quantitative PCR and the 2(-Delta Delta C(T)) method. Methods 25(4):402–408, PMID: 11846609, https://doi.org/10.1006/meth.2001.1262.
Mattos Y, Stotz WB, Romero MS, Bravo M, Fillmann G, Castro IB. 2017. Butyltin contamination in northern Chilean coast: is there a potential risk for consumers? Sci Total Environ 595:209–217, PMID: 28384577, https://doi.org/10.1016/j.scitotenv.2017.03.264.
Menke A, Casagrande S, Geiss L, Cowie CC. 2015. Prevalence of and trends in diabetes among adults in the United States, 1988–2012. JAMA 314(10):1021–1029, PMID: 26348752, https://doi.org/10.1001/jama.2015.10029.
Merkord J, Jonas L, Weber H, Kröning G, Nizze H, Hennighausen G. 1997. Acute interstitial pancreatitis in rats induced by dibutyltin dichloride (DBTC): pathogenesis and natural course of lesions. Pancreas 15(4):392–401, PMID: 9361094.
Merkord J, Weber H, Sparmann G, Jonas L, Hennighausen G. 1999. The course of pancreatic fibrosis induced by dibutyltin dichloride (DBTC). Ann N Y Acad Sci 880:231–237, PMID: 10415868.
Milton FA, Lacerda MG, Sinoti SBP, Mesquita PG, Prakasan D, Coelho MS, et al. 2017. Dibutyltin compounds effects on PPARγ/RXRα activity, adipogenesis, and inflammation in mammalians cells. Front Pharmacol 8:507, PMID: 28824431, https://doi.org/10.3389/fphar.2017.00507.
Mimoto MS, Nadal A, Sargis RM. 2017. Polluted pathways: mechanisms of metabolic disruption by endocrine disrupting chemicals. Curr Environ Health Rep 4(2):208–222, PMID: 28432637, https://doi.org/10.1007/s40572-017-0137-0.
Miura Y, Kato M, Ogino K, Matsui H. 1997. Impaired cytosolic Ca2+ response to glucose and gastric inhibitory polypeptide in pancreatic beta-cells from triphenyltin-induced diabetic hamster. Endocrinology 138(7):2769–2775, PMID: 9202216, https://doi.org/10.1210/endo.138.7.5234.
Morton GJ, Meek TH, Schwartz MW. 2014. Neurobiology of food intake in health and disease. Nat Rev Neurosci 15(6):367–378, PMID: 24840801, https://doi.org/10.1038/nrn3745.
Myers MG, Jr, Leibel RL, Seeley RJ, Schwartz MW. 2010. Obesity and leptin resistance: distinguishing cause from effect. Trends Endocrinol Metab 21(11):643–651, PMID: 20846876, https://doi.org/10.1016/j.tem.2010.08.002.
Newbold RR, Padilla-Banks E, Jefferson WN, Heindel JJ. 2008. Effects of endocrine disruptors on obesity. Int J Androl 31(2):201–208, PMID: 18315718, https://doi.org/10.1111/j.1365-2605.2007.00858.x.
Ng M, Fleming T, Robinson M, Thomson B, Graetz N, Margono C, et al. 2014. Global, regional, and national prevalence of overweight and obesity in children and adults during 1980–2013: a systematic analysis for the global burden of disease study 2013. Lancet 384(9945):766–781, PMID: 24880830, https://doi.org/10.1016/S0140-6736(14)60460-8.
Noda T, Morita S, Baba A. 1993. Teratogenic effects of various di-n-butyltins with different anions and butyl(3-hydroxybutyl)tin dilaurate in rats. Toxicology 85(2–3):149–160, PMID: 8303710.
Ogden CL, Carroll MD, Kit BK, Flegal KM. 2014. Prevalence of childhood and adult obesity in the United States, 2011-2012. JAMA 311(8):806–814, PMID: 24570244, https://doi.org/10.1001/jama.2014.732.
Ogurtsova K, da Rocha Fernandes JD, Huang Y, Linnenkamp U, Guariguata L, Cho NH, et al. 2017. IDF Diabetes Atlas: global estimates for the prevalence of diabetes for 2015 and 2040. Diabetes Res Clin Pract 128:40–50, PMID: 28437734, https://doi.org/10.1016/j.diabres.2017.03.024.
Rantakokko P, Main KM, Wohlfart-Veje C, Kiviranta H, Airaksinen R, Vartiainen T, et al. 2014. Association of placenta organotin concentrations with growth and ponderal index in 110 newborn boys from Finland during the first 18 months of life: a cohort study. Environ Health 13(1):45, PMID: 24899383, https://doi.org/10.1186/1476-069X-13-45.
Sadiki AI, Williams DT, Carrier R, Thomas B. 1996. Pilot study on the contamination of drinking water by organotin compounds from PVC materials. Chemosphere 32(12):2389–2398, PMID: 8653382.
Shoucri BM, Martinez ES, Abreo TJ, Hung VT, Moosova Z, Shioda T, et al. 2017. Retinoid x receptor activation alters the chromatin landscape to commit mesenchymal stem cells to the adipose lineage. Endocrinology 158(10):3109–3125, PMID: 28977589, https://doi.org/10.1210/en.2017-00348.
Soriano S, Alonso-Magdalena P, García-Arévalo M, Novials A, Muhammed SJ, Salehi A, et al. 2012. Rapid insulinotropic action of low doses of bisphenol-A on mouse and human islets of Langerhans: role of estrogen receptor β. PLoS One 7(2):e31109, PMID: 22347437, https://doi.org/10.1371/journal.pone.0031109.
Suvorov A, Vandenberg LN. 2016. To cull or not to cull? Considerations for studies of endocrine-disrupting chemicals. Endocrinology 157(7):2586–2594, PMID: 27175970, https://doi.org/10.1210/en.2016-1145.
Tabak AG, Herder C, Rathmann W, Brunner EJ, Kivimaki M. 2012. Prediabetes: a high-risk state for diabetes development. Lancet 379:2279–2290.
Tontonoz P, Spiegelman BM. 2008. Fat and beyond: the diverse biology of PPARgamma. Annu Rev Biochem 77:289–312, PMID: 18518822, https://doi.org/10.1146/annurev.biochem.77.061307.091829.
Yanik SC, Baker AH, Mann KK, Schlezinger JJ. 2011. Organotins are potent activators of PPARgamma and adipocyte differentiation in bone marrow multipotent mesenchymal stromal cells. Toxicol Sci 122(2):476–488, PMID: 21622945, https://doi.org/10.1093/toxsci/kfr140.
Yao TP, Forman BM, Jiang Z, Cherbas L, Chen JD, McKeown M, et al. 1993. Functional ecdysone receptor is the product of EcR and Ultraspiracle genes. Nature 366(6454):476–479, PMID: 8247157, https://doi.org/10.1038/366476a0.
Zeng W, Pirzgalska RM, Pereira MM, Kubasova N, Barateiro A, Seixas E, et al. 2015. Sympathetic neuro-adipose connections mediate leptin-driven lipolysis. Cell 163(1):84–94, PMID: 26406372, https://doi.org/10.1016/j.cell.2015.08.055.
Zhang H, Liu B, Xu XF, Jiang TT, Zhang XQ, Shi YL, et al. 2016. Pathophysiology of chronic pancreatitis induced by dibutyltin dichloride joint ethanol in mice. World J Gastroenterol 22(10):2960–2970, PMID: 26973392, https://doi.org/10.3748/wjg.v22.i10.2960.
Zhu J, Janesick A, Wu L, Hu L, Tang W, Blumberg B, et al. 2017. The unexpected teratogenicity of RXR antagonist UVI3003 via activation of PPARγ in Xenopus tropicalis. Toxicol Appl Pharmacol 314:91–97, PMID: 27894914, https://doi.org/10.1016/j.taap.2016.11.014.